Redox switching of Prussian blue thin films investigated by ac-electrogravimetry

Loan To Thi Kim, Claude Gabrielli, Hubert Perrot, J. Garcia-Jareno, F. Vicente

Redox switching of Prussian Blue Thin Films Investigated by *ac*-electrogravimetry.

L. To Thi Kim[1,2], C. Gabrielli[1,2], H. Perrot[1,2,*],
J. Garcia-Jareno[3], F Vicente[3].

1-CNRS, UPR 15, LISE, F-75252, Paris, France
2-UPMC Univ. Paris 06, UPR15, LISE, F- 75252 Paris, France
3-Depto de Quimica-Fisica, Univ. Valencia, Burjassot, Spain

ABSTRACT

In this paper, the redox switching behaviour of Prussian Blue (PB) in KCl environment at pH 2.5 and 5.4 was investigated by using *ac*-electrogravimetry in a potential range around the conversion of PB to ES (Everitt Salt). This technique allows the electrochemical impedance and a mass-potential transfer function to be simultaneously measured. From the impedance the charge-potential transfer function is calculated. A model of the PB film, is presented, it takes into account the porous structure of the material, the insertion of two cations on the pore wall, and the electronic charge transfer from the electrode. A fitting procedure was employed to obtain the kinetic parameters.

Attractive information extracted from the impedance concerns the porosity of the PB film which is related to the zeolitic nature of the film. The resistivity of the pore depends obviously on the electrolyte conductance and changes with respect to the potential with a minimum, in the vicinity of the PB↔ES conversion potential.

Ac-electrogravimetry and the charge-potential transfer function gave essentially information on the kinetics of the ionic transfer. Thanks to the model of electroactive porous films and the digital fitting procedure, for the first time, the two cations K^+ and H_3O^+ are identified with well separated kinetics for each cation. Several attractive informations were reached. First, it confirms that ionic transfer at the film/electrolyte interface limits the kinetics of the film reduction or oxidation as electronic transfer at the electrode/film interface is faster. Moreover, the rates of the electronic and ionic transfer kinetics vary with the potential. They are faster around the potential where the PB↔ES conversion occurs. It was confirmed that charge compensation occurs only by K^+ and H_3O^+ movements whatever the pH of the solution. However, H_3O^+ transfer kinetics is faster than K^+ transfer, whatever the KCl concentration, and the role of H_3O^+ is more important for large KCl concentrations where the

process is more limited by the kinetics of the hydronium ions. In addition, in these situations, even if ionic transfer is also accelerated the global charge transfer is nevertheless more controlled by electronic transfer

KEYWORDS: *ac*-electrogravimetry; Prussian Blue; Porosity; ionic transfer; electronic transfer

* Corresponding author

1 - INTRODUCTION

Prussian Blue (PB) or iron hexacyanoferrate is considered as the first synthesised coordination compound. Although it has been studied for 270 years, it is still a research topic of high interest because of its numerous interesting properties as electrochromism, ion exchanger, and photomagnetic properties which allow applications in electrocatalysis, electrochromic or electronic devices, and batteries. PB films can be generated by chemical [1-2] or electrochemical [3-4] ways, often from an aqueous solution of a $FeCl_3$ and $K_3Fe(CN)_6$ mixture. PB was deposited at an electrode surface for the first time by V.D. Neff [5] The films obtained after the deposit are under the so-called insoluble form with formula $Fe_4^{3+}[Fe^{2+}(CN)_6]_3.mH_2O$. The films are converted under the so-called soluble form $KFe^{3+}[Fe^{2+}(CN)_6].mH_2O$ after a few voltammetric cycles in a KCl solution.

The first structure of PB has been proposed by Keggin and Miles [6] from X rays studies. In the $Fe_4^{3+}[Fe^{2+}(CN)_6]_3.mH_2O$ crystalline structure, Fe^{3+} ions (high spin iron) and Fe^{2+} iron (low spin iron) are alternatively localized on the centered faces of the cubic lattice in a way that the Fe^{3+} ions are surrounded by nitrogen atoms and the Fe^{2+} ions are surrounded by carbon atoms. During the conversion between the insoluble and soluble forms, the film loses a quarter of the Fe^{3+} ions (high spin iron) which are substituted by the K^+ cations. In addition, it has been shown that the soluble structure contains between 14 and 16 water molecules by elementary mesh unit [7]. In the PB film, two types of water molecules have been observed by neutron diffractometry [8] : 6 water molecules are coordinated with the $Fe(CN)_6^{4+}$ vacancies and the others occupy interstitial sites without any coordination. Ganguli *et al.* [9] have studied the dehydration process of PB by thermogravimetry. They have identified three different hydration states and an anhydrous one. The decomposition occurs at temperature greater than 150°C. The hydration degree of the films depends on the temperature and humidity of the environment. It was observed that about 90% of water is eliminated by a 150°C heating. When dehydrated PB is reexposed to ambient air, it takes again the same hydration amount.

The PB soluble film [10] is reduced to the uncoloured form, called Everitt salt (ES), in a KCl solution:

$$\underset{\text{PB}}{KFe^{3+}Fe^{2+}(CN)_6} + e^- + K^+ \leftrightarrow \underset{\text{ES}}{K_2Fe^{2+}Fe^{2+}(CN)_6} \qquad (1)$$

Itaya *et al.* [10] have shown by spectroelectrochemistry that only some cations can migrate through the PB film because of its zeolitic and nanoporous structure (pore diameter:

3,2 Å). Thus, this structure is permeable to cations with radii (r) less than 1,6 Å, such as K^+ (r = 1,25 Å), Rb^+(r = 1,18 Å), Cs^+ (r = 1,19 Å), and NH_4^+ (r = 1,25 Å) but cations with greater radii such as Li^+(r = 2,39 Å) and Mg^+(r = 3,47 Å) are blocked. However, the Na^+ cation (r = 1.84 Å) can be also inserted in an amorphous PB film formed at larger cathodic currents. Garcia-Jareno *et al.* [11] have also shown by *ac*-electrogravimetry that the Na^+ cation is partially dehydrated before to be transported through the zeolitic channels of PB during an electrochemical process.

The use of an electrochemical quartz microbalance (EQCM) was very efficient to understand the ionic transfer which is involved in the redox process of a PB film. It has been shown that the insertion/expulsion process of the alcaline cation is more complicated than what is presented in Equation (1). Feldman *et al.* [12] have proposed that the insertion of the alcaline cation is accompanied by the proton insertion or by the expulsion of solvent, the measured apparent molar mass is the average of the proton and the alcaline cation masses. Later, by a mirage effect technique [13], the cation flux has been also found in competition with the proton flux. By using the electrochemical impedance technique, Garcia-Jareno et *al.* [14,15] have demonstrated that protons play an important role in the kinetics of the electron transport by *hopping* and that the solvent contribution is necessary to accompany counter ions. Kim *et al.* [16] have reached the same conclusion in 2001 by cyclic electrogravimetry. These authors have reported that the insertion/expulsion process of the alcaline cation is accompanied by the transfer of free solvent (H_2O) in the K_2SO_4 0.5M - pH 6.3 medium. Whereas, in the same solution at pH 2.7, the K^+ ion transfer is not only accompanied by solvent transfer but is also in competition with the transfer of the solvated proton. The first investigations of the PB films in KCl at pH 2.7 by *ac*-electrogravimetry, [17] have allowed information on the insertion kinetics of the K^+ and H_3O^+ cations to be obtained at various potentials. When the film is polarized in cathodic regime, only the K^+ cation participation was shown through the determination of a molar mass equal to 39 $g.mol^{-1}$ but the solvated proton is mainly involved in the charge compensation towards the more positive potentials where a molar mass equal to 19 $g.mole^{-1}$ was obtained. At intermediate potentials, the average molar mass changes between 19 and 39 $g.mole^{-1}$. It is noticeable that in these works, the kinetics of the two cations were not separated and only a global ionic transfer was taken into account. *Ac*-electrogravimetry was also recently used to examine the electrochemical behavior of hybrid inorganic-organic electroactive films [18] or bilayers films employed for PEM characterization [19].

This work was aimed at studying the kinetics of PB in KCl - medium at pH 2.5 and pH 5.4. In addition to the simpler model used in the previous works the electronic transfer at the electrode/film interface and the nanoporous nature of PB will be taken into account. Thanks to a more accurate experimental device and a fitting procedure to a more involved model, we were able to separate the kinetics of K^+ and H_3O^+ cations in the charge compensation process.

2 - MODEL

In this part, we shall give a model of porous electroactive films which will be applied in the following to explain the PB film redox behaviour.

2.1 - Generalities on porous electrodes

In 1948 V. S. Daniel-Bekh and then in 1960 J. Euler and W. Nonnenmacher [20] have been the first to model porous electrodes. Later, a model based on a transmission line has been developed by de Levie [21,22,23]. The simplest models consider a cylindrical pore with length L and radius r_0. The pore wall is supposed to react with the electrolytic solution. The behaviour of this pore called active differs from the pores called passive where reactions occur only at the pore end. The current flowing through the pore provokes an ohmic drop related to the resistivity of the electrolyte in the pore. So, as a part of the current passes through the pore wall, the local current varies with the pore depth x. This is the cause of the particular behaviour of porous electrodes: on the one hand, a potential and current distribution is observed in the pore and, on the other hand, an axial concentration distribution is also observed if reactions occur on the pore wall.

Therefore, the general modelling is based on three fundamental relationships which describe the electrode behaviour:

- *Ohmic drop in the pore.* At a distance x from the pore entrance, an elementary ohmic drop can be considered:

$$de(x) = -\rho_2 . i(x) . dx \tag{2}$$

where $de(x)$ (V) and $i(x)$ (A.cm^{-2}) are the potential and current at a distance x from the pore entrance, ρ_2 (Ω.cm) is the resistivity of the electrolyte in the pore and dx is a distance increment.

- *Interfacial kinetics on the pore wall* At a distance x from the pore entrance, a current, $di(x)$ related to the electrochemical reaction on the pore wall can be written for a simple reaction:

$$di(x) = -K.c(x).dx \tag{3}$$

where K is the rate constant which depends on the local potential *e(x)* and *c(x)* is the local concentration.

- *Diffusion in the pore* At a distance *x* from the pore entrance, a variation of the active species concentration can be written following the Fick law:

$$\frac{dc}{dt} = D\frac{\partial^2 c}{dx^2} - K_P.c(x) \tag{4}$$

where K_p is the rate constant related to a reaction in the volume of the pore.

However, to take into account the transport of the species is very complicated. In fact, this transport can be decomposed between an axial component which brings the reactive species from the « mouth » of the pore to the reaction zone and a radial component which goes from the pore axis to bring the species up to the pore wall where the reaction occurs. The transport was considered as radial by de Levie [21,22,23] or axial by Keddam et al. [24]. Usually, to take into account both ohmic drop and diffusion needs digital calculation. So, J. Newman and C. W. Tobias [25], C. Cachet and R. Wiart [26] and Paasch et al. [27] have given such a solution.

Another approach has been proposed recently by La Mantia et al. [28] where a coupling between the local potential and concentration is taken into account by assuming that the potential difference in the pore depends both on the ohmic drop (which depends on the local current density) and a diffusion ohmic drop (which depends on the concentration gradient).

Also, by considering porous films, Barker [29], Albery [30], Buck [31, 32] et Paasch [33, 34, 35, 36] have calculated the electrochemical impedance of an electrode/film/electrolyte system.

By assuming that the axial concentration gradient is negligible, i.e. *c(x)* is a constant, R. de Levie has given the pore impedance, $Z_P(\omega)$, per pore cross section unit, under the form:

$$Z_P(\omega) = \sqrt{\rho_2 Z_0(\omega)}\, coth\left[L\sqrt{\frac{\rho_2}{Z_0(\omega)}}\right] \tag{5}$$

where $Z_0(\omega)$ is the faradaic impedance relative to the electrochemical reaction of the species at the electrolyte/pore wall which will be calculated below.

Then the penetration depth of the electrical perturbation signal can be defined such as

$$\lambda = \sqrt{\frac{Z_0(\omega)}{\rho_2}} \tag{6}$$

In the low frequency range ($\omega \to 0$) and $Z_0 » \rho_2$, (i. e. $L << \lambda$, which means that the potential perturbation goes to the end of the pore), then $\coth\left[L\sqrt{\frac{\rho_2}{Z_0(\omega)}}\right] = \frac{1}{L\sqrt{\frac{\rho_2}{Z_0(\omega)}}} + \frac{L\sqrt{\frac{\rho_2}{Z_0(\omega)}}}{3}$, the pore impedance becomes : $Z_{P_{BF}}(\omega) = \frac{Z_0(\omega)}{L} + \frac{\rho_2 L}{3}$. Hence, in the low frequency range, the impedance of a cylindrical pore is equal to that of the flat electrode of same area as the developed pore surface, but with a shift of the real part equal to the third of the ohmic drop of the pore $\Omega = \rho_2 L$.

In the high frequency range ($\omega \to \infty$) and $Z_0 « \rho_2$, (i. e. $L >> \lambda$, which means that the potential perturbation does not practically enter the pore) then $\coth\left[L\sqrt{\frac{\rho_2}{Z_0(\omega)}}\right] = 1$ therefore $Z_p(\omega) = \sqrt{\rho_2 Z_0(\omega)}$ does not depend on the pore length. It is called the impedance of a semi-infinite cylindrical pore.

Therefore, impedance measurements allow the pore texture of a porous electrode (equivalent pore radius, r_0, and pore length, L) and the resistivity of the electrolyte in the pore to be characterized.

2.2 - Local impedance due to the ionic transfer : $Z_0(\omega)$

Ionic transfer occurs at the film/electrolyte interface [17,37,38] The flux of species *i* (*a*: anion, *c*: cation, *s*: solvent), J_i, is considered as positive if the species is expulsed from the film:

$$J_i > 0 \quad \text{pour} \quad x > 0 \tag{7}$$

If both cations, anions and solvent are involved in the charge compensation process, the associated mass variation, Δm and the electric charge variation per surface unit, Δq, which flows through the electrode/film interface, are equal to:

$$\Delta m = m_c \xi_c + m_a \xi_a + m_s \xi_s \tag{8}$$

$$\Delta q = -F(\Delta \xi_c - \Delta \xi_a) \tag{9}$$

where m_i and ξ_i are the molar mass and the quantity of moles of species i exchanged, respectively.

The general doping mechanism of an electroactive film by a cation or an anion can be described by the following reactions:

$$< P_c > + e^- + C^+ \underset{k_c'}{\overset{k_c}{\rightleftarrows}} < P_c, C^+ > \qquad \text{and} \qquad < P_a > + A^- \underset{k_a}{\overset{k_a'}{\rightleftarrows}} < P_a, A^- > + e^- \quad (10)$$

where the $< P_i >$ are free electroactive sites of the film available for cations $(i = c)$ and anions $(i = a)$, $<P_i,C^+>$, and $<P_i,A^->$ the cations and anions inserted in the film associated to the sites.

Consequently, the instantaneous molar flux of species i (c, a, or s) is $J_i = \frac{d\xi_i}{dt}$ and the concentration of species i in thin films of thickness d_f can be written under the form:

$$\xi_i = d_f C_i \quad (11)$$

By using the laws of the heterogeneous kinetics and reactions (10), the flux J_i of cations and anions are:

$$J_a(d_f) = -d_f \frac{dC_a}{dt} = k_a (C_a - C_{a\min}) - k_a' (C_{a\max} - C_a) C_{asol} \quad (12)$$

$$J_c(d_f) = -d_f \frac{dC_c}{dt} = k_c' (C_c - C_{c\min}) - k_c (C_{c\max} - C_c) C_{csol} \quad (13)$$

By using the Hillman solvation model [39] , the same relationship can be used for the solvent flux:

$$J_s(d_f) = -d_f \frac{dC_s}{dt} = k_s' (C_s - C_{s\,min}) - k_s (C_{s\,max} - C_s) \quad (14)$$

where

- C_i is the concentration of species i in the film, C_{isol} is the concentration of species i in the solution by assuming that the diffusion of the ions in solution does not limit the global kinetics;
- the term $[C_{imax} - C_i]$ is the concentration in free sites for species i at time t, where C_{imax} is the maximum concentration of the free sites in the film for species i ;
- the term $[C_i - C_{imin}]$ is the concentration of species i in the film bulk at time t, where C_{imin} is the minimum concentration of species i in the film.

Finally, the kinetic constants depend on potential under the form:

$$k_i^{'} = k_{i0}^{'} e^{\left[b_i^{'}\left(E-E_i^{o}\right)\right]} \tag{15}$$

$$k_i = k_{i_o} e^{\left[b_i\left(E-E_i^{o}\right)\right]} \tag{16}$$

where E is the potential, E_i° is the apparent normal potential, (E- E_i°) is the overvoltage, k_{i0}, k'_{i0}, b_{i0} and b'_{i0} are constants.

2.2.1 - *Boundary limits*

By considering that the electrolyte in the pore contains only one type of cation and one type of anion and by using the Faraday law, the current density, $j_{F,}$ at the film/electrolyte interface (at the pore wall which is characterized by an equivalent thickness d_f)

$$-J_a(d_f) + J_c(d_f) = \frac{j_F}{F} \tag{17}$$

On the contrary, at the electrode/film interface ($x=0$), where only electrons are exchanged, the flux of ions and solvent are:

$$J_a = J_c = J_s = 0 \tag{18}$$

Now, the insertion laws can be determined in steady and dynamic states.

2.2.2 - *Steady state*

At steady state, the system is at equilibrium and the flux J_i are zero. Then, the steady state concentrations (insertion laws) are from equations (12-13-14).

$$C_i(E) = \frac{C_{i\,max} e^{[(b_i^{'}-b_i)(E-E_i^{o}-E_i)]} + C_{i\,min}}{1 + e^{[(b_i^{'}-b_i)(E-E_i^{o}-E_i)]}} \tag{19}$$

by defining E_i such as $C_{isol} \cdot \frac{k_{i0}^{'}}{k_{i0}} = e^{-(b_i-b_i^{'})\cdot E_i}$.

2.2.3 - *Dynamic regime*

Under the effect of a potential sinusoidal perturbation with low amplitude, ΔE, imposed to the electrode/film/electrolyte system, sinusoidal fluctuations of concentration, ΔC_i, and flux, ΔJ_i, are observed such as:

$$\Delta J_i = -d_f \frac{dC_i}{dt} = -j\omega d_f \Delta C_i \tag{20}$$

On the other hand, the expression of the global insertion/expulsion flux, ΔJ_i, which depends on the concentration and potential perturbations, at the film/electrolyte interface is:

$$\Delta J_i = \frac{\partial J_i}{\partial C_i}\Bigg)_E \Delta C_i + \frac{\partial J_i}{\partial E}\Bigg)_{C_i} \Delta E = K_i \Delta C_i(d_f) + G_i \Delta E \tag{21}$$

where

$$K_a = \left(\frac{\partial J_a}{\partial C_a}\right)_E = k_a + k'_a C_{a_{sol}} \tag{22}$$

$$K_c = \left(\frac{\partial J_c}{\partial C_c}\right)_E = k'_c + k_c C_{c_{sol}} \tag{23}$$

$$G_a = \left(\frac{\partial J_a}{\partial E}\right)_{C_a} = \left[b_a k_a \left(C_a - C_{a_{\min}}\right) - b_a{}' k_a{}' (C_{a_{\max}} - C_a) C_{a_{sol}} \right] \tag{24}$$

$$G_c = \left(\frac{\partial J_c}{\partial E}\right)_{C_c} = \left[b'_c k'_c \left(C_c - C_{c_{\min}}\right) - b_c k_c (C_{c_{\max}} - C_c) C_{c_{sol}} \right] \tag{25}$$

K_i is the time constant of the kinetics of the species global transfer; G_i is the inverse of the transfer resistance of the species at the film/solution interface (where i is the cation c, the anion a or the solvent s). From Equations (20-21) the insertion law can be written under the form:

$$\frac{\Delta C_i}{\Delta E}(\omega) = \frac{-G_i}{j\omega d_f + K_i} \tag{26}$$

which gives the concentration response to a potential perturbation.

2.3 - Model of electroactive porous films with two inserted cations

To study the behaviour of the electroactive porous films by ac-electrogravimetric technique, a model will be presented now. It is based on the insertion/expulsion of two different cations, c_1 and c_2, in independent sites in PB films, P_{c_1} and P_{c_2}, such as:

$$< P_{c_1} > + e^- + C_1^+ \underset{k'_{c1}}{\overset{k_{c1}}{\rightleftarrows}} < P_{c_1}, C_1^+ > \qquad\qquad < P_{c_2} > + e^- + C_2^+ \underset{k'_{c2}}{\overset{k_{c2}}{\rightleftarrows}} < P_{c_2}, C_2^+ > \tag{27}$$

To simplify the derivation, a few hypotheses are used:

- ✓ As the electronic transfer is not infinitely fast, an electronic transfer resistance, R_e, is considered in parallel on a capacity across the electrode/film interface.
- ✓ Ion transport in the solution and in the electroactive film is fast.

2.3.1 - *Electrochemical impedance* $\frac{\Delta E}{\Delta I}(\omega)$

2.3.1.1 - Faradaic impedance related to ionic transfer

In dynamic regime, the perturbation ΔE leads to a variation of the charge in the film by considering that the two cations, c_1 and c_2, are involved in the charge compensation process using Equations (10). In addition, the faradaic current density is such that $\Delta I_F = j\omega\Delta q$. By using relationship (9) and by dividing by ΔE, the Faradaic admittance is calculated for the insertion/expulsion of the two cations:

$$\frac{\Delta I_F}{\Delta E} = -j\omega F d_f \left(\frac{\Delta C_{c_1}}{\Delta E} + \frac{\Delta C_{c_2}}{\Delta E} \right) \tag{28}$$

Moreover, Equation (26) relative to the insertion law allows the impedance to be calculated:

$$\frac{1}{Z_{Fc_i}} = -j\omega F d_f \frac{\Delta C_{c_i}}{\Delta E} = j\omega F d_f \frac{G_{c_i}}{j\omega d_f + K_{c_i}} \tag{29}$$

where Z_{Fi} is the Faradaic impedance relative to the ionic transfer of cation *i*, for which $G_i > 0$

By using Equations (26 and 28), the faradaic impedance, $Z_F(\omega)$ relative to the global ionic transfer of the electroactive film for two species (cation and anion) involved in the charge compensation is:

$$Z_F(\omega) = \frac{\Delta E}{\Delta I_F}(\omega) = \frac{1}{j\omega d_f F \left[\frac{G_{c_1}}{j\omega d_f + K_{c_1}} + \frac{G_{c_2}}{j\omega d_f + K_{c_2}} \right]} \tag{30}$$

2.3.1.2 - Electrochemical impedance of a porous electroactive film

To simplify, the electroactive film is supposed to be constituted by cylindrical pores full of electrolyte where the insertion/expulsion reactions occurs on the wall (Figure 1).

Using the De Levie model given above, the impedance of the pore, $Z_P(\omega)$, is:
[40]

$$Z_P(\omega) = \sqrt{\rho_2 Z_0(\omega)}\, coth\left[L\sqrt{\frac{\rho_2}{Z_0(\omega)}} \right] \tag{31}$$

where

$$Z_0(\omega) = \frac{1}{j\omega C_d + \frac{1}{Z_F(\omega)}} \tag{32}$$

is the Faradaic impedance per surface unit of pore wall, relative to the ionic transfer of species Z_{Fi} (i: cations or anions) in parallel with a double layer capacity C_d at the pore wall/electrolyte interface.

$$Z_0(\omega) = \frac{1}{j\omega C_d + j\omega d_f F\left[\frac{G_{c_1}}{j\omega d_f + K_{c_1}} + \frac{G_{c_2}}{j\omega d_f + K_{c_2}}\right]} \tag{33}$$

2.3.1.3 - *Global electrochemical impedance*

The global electrochemical impedance of the porous electroactive is the sum of the impedance related to the electronic transfer at the electrode/film interface (contact of PB with the metallic electrode), Z_e, the impedance of the pore, Z_P, and the solution resistance, R_s:

$$Z(\omega) = R_s + Z_e + Z_P = R_s + \frac{1}{\frac{1}{R_e} + j\omega C_e} + \sqrt{\rho_2 Z_0(\omega)}\, coth\left[L\sqrt{\frac{\rho_2}{Z_0(\omega)}}\right] \tag{34}$$

where R_e is the electronic transfer resistance and C_e the capacity of the electrode/film interface.

At low frequency: $\omega \to 0$, $Z_P(\omega) = \frac{Z_0(\omega)}{L} + \frac{\rho_2 L}{3}$, (35)

and the global electrochemical impedance is then:

$$Z_{BF}(\omega) = R_s + \frac{1}{\frac{1}{R_e} + j\omega C_e} + \frac{Z_0}{L} + \frac{\rho_2 L}{3} \tag{36}$$

2.3.2 - Electrogravimetric transfer function $\frac{\Delta m}{\Delta E}(\omega)$

The ΔE perturbation leads to a change of the charge compensation related to the species going in and out (cation, anion, and solvent) at the mouth of the pore. By considering that the mass response to the electrical sine wave perturbation occurs only in the low frequency range, the mass variation Δm, following Equation (8), dividing by ΔE, and using relationship (11), the function $\frac{\Delta m}{\Delta E}(\omega)$ relative to the insertion/expulsion of the cations c_1 and c_2, and eventually solvent, becomes:

$$\frac{\Delta m}{\Delta E}(\omega) = d_f\left[m_{c_1}\frac{\Delta C_{c_1}}{\Delta E} + m_{c_2}\frac{\Delta C_{c_2}}{\Delta E} + m_s\frac{\Delta C_s}{\Delta E}\right] \tag{37}$$

In Equation (38), the global electrogravimetric transfer function per electrode surface unit taking into account all the involved species (cation, anion and solvent) is:

$$\frac{\Delta m}{\Delta E}(\omega) = -d_f \left(m_{c_1} \frac{G_{c_1}}{j\omega d_f + K_{c_1}} + m_{c_2} \frac{G_{c_2}}{j\omega d_f + K_{c_2}} + m_s \frac{G_s}{j\omega d_f + K_s} \right) \quad (38)$$

2.4 - Experimental data treatment

The experimental data were fitted to the model of the porous electroactive film described above to obtain the kinetic parameters by using a digital fitting procedure based on a Least Square Method (WNCLNSF software developed by J. Garcia-Jareno and F. Vicente, Univ. Valencia, Spain). The three transfer functions: electrochemical impedance, charge/potential transfer function, and the electrogravimetric transfer function were separately used.

2.4.1 - *Electrochemical impedance*

The fitting procedure applied to the electrochemical impedance in the frequency range (0.01Hz – 60 kHz) and by considering only a global ionic transfer (where two cations are considered at the same time) with impedance Z_t, allows informations relative to the electronic and the global ionic transfer and the porosity of the electroactive film to be obtained. Diffusion is neglected as the film is very thin and typical responses, ie 45° slopes, were not observed for the EIS responses.

By taking into account the electrolyte resistance, R_s, and by using Equation (35), the electrochemical impedance of the electroactive film is equal to:

$$Z(\omega) = R_s + Z_p + Z_e \quad (39)$$

$$\text{where } Z_P(\omega) = \sqrt{\rho_2 Z_0(\omega)}\, coth\left[L\sqrt{\frac{\rho_2}{Z_0(\omega)}} \right], \; Z_0(\omega) = \frac{1}{j\omega C_d + \frac{1}{Z_t}}, \quad (40)$$

$$Z_e(\omega) = \frac{1}{\frac{1}{R_e} + j\omega C_e} \text{ and } Z_t(\omega) = R_t + \frac{1}{j\omega C_t}$$

where R_t is the ionic transfer resistance and C_t is the global insertion capacity.

As $Z_P(\omega)$ can be also be written under the form:

$$Z_P(\omega) = \sqrt{\rho_2 L \frac{Z_0(\omega)}{L}} \coth\left[\sqrt{\frac{\rho_2 L}{\frac{Z_0(\omega)}{L}}} \right] \quad (41)$$

where $\frac{Z_0(\omega)}{L} = \frac{1}{j\omega C_d L + \frac{1}{\frac{Z_{Fi}}{L}}}$

and $\frac{Z_{Fi}}{L} = \frac{R_t}{L} + \frac{1}{j\omega C_t L}$

Therefore, all the quantities will be given per pore length unit.

Nine parameters R_s, L, ρ_2, R_i, C_i, C_d, C_e, R_e (and a_m when a CPE is considered relatively to C_d) are obtained thanks to the electrochemical impedance. The free parameters are R_s, $\rho_2 L$, R_i/L, C_iL, C_dL, C_e, R_e.

It is noticeable that for the electrochemical impedance, only one Faradaic impedance, Z_t, relative to the global ionic transfer which represents all the charged species participating to the charge compensation process is taken into account to simplify the fitting procedure. Thus two global quantities R_i and C_i are only obtained. The film response in the low frequency range, which is related to the ionic transfer, will be more precisely interpreted below by using the two other transfer functions. In this way, the kinetic constants K_i and G_i of the involved cations will be separately estimated.

2.4.2 - *Charge/potential transfer function*

The charge/potential transfer function, calculated from the experimental electrochemical impedance, is equal to:

$$\frac{\Delta q}{\Delta E}(\omega) = \frac{1}{j\omega}\frac{1}{Z_0} \tag{42}$$

gives information on the ionic transfer. For the fitting, it can be conveniently written under the form:

$$\frac{\Delta q}{\Delta E}(\omega) = C_d + \frac{1}{j\omega}\sum_i \left(\frac{1}{R_i + \frac{1}{j\omega C_i}} \right) \tag{43}$$

By using Equation (31),

$$\frac{1}{Z_{Fi}} = j\omega.F.d_f \frac{G_i}{j\omega d_f + K_i}\ , \tag{44}$$

the relationships between R_i, C_i and G_i, K_i can be deduced for all the involved species:

$$Z_{Fi} = R_i + \frac{1}{j\omega C_i} = \frac{1}{FG_i}\left(1 + \frac{K_i}{j\omega d_f}\right) \quad (44)$$

therefore $$G_i = \frac{1}{FR_i} \quad \text{and} \quad K_i = d_f \frac{1}{R_i C_i} \quad (45)$$

For each charged species, three parameters R_i, C_i (and a_f when the insertion capacity is considered as a CPE) have to be fitted by considering only the low frequency range (0.01 Hz – 100 Hz) where $\frac{\Delta q}{\Delta E}$ and $\frac{\Delta m}{\Delta E}$ are of interest (which correspond to the quasi-vertical capacitive part of the electrochemical impedance). As soon as these three parameters are determined, they are used for the fitting of the electrogravimetric transfer function.

2.4.3 - *Electrogravimetric transfer function*

For each species, four parameters R_i, C_i, a_f *et* m_i have to be determined. Equation (39) is used for the fitting in the same frequency range of $\frac{\Delta q}{\Delta E}$. Finally, the kinetic parameters K_i and G_i are determined from the components R_i and C_i of the equivalent circuit.

$$\frac{\Delta m}{\Delta E}(\omega) = \sum \frac{m_i}{F} \frac{1}{j\omega Z_i} = L \sum_i \frac{m_i}{F} \frac{1}{j\omega\left(R_i + \frac{1}{j\omega C_i}\right)} = d_f \sum_i m_i \frac{G_i}{j\omega d_f + K_i} \quad (47)$$

In all these fitting procedures, the thickness of the film was taken equal to 100 nm as determined experimentally (see below).

3 - EXPERIMENTAL

The PB films were obtained by electrodeposit, in galvanostatic mode, on the gold electrode of a quartz resonator (AWS Company, Spain) acting as a classical working electrode, from a 0.02M $K_3(Fe(CN)_6)$ (Prolabo-93.3%), 0.02M $FeCl_3$ (Prolabo-99.4%) and 0.01M HCl (Prolabo-37%) solution. A 40 µA cm^{-2} cathodic current was applied during 150 s, to obtain a 100 nm thick PB film. The film thickness was estimated by SEM measurements. The film was then cycled 15 times in aqueous medium containing 0.5M KCl (Prolabo-99.7%) pH 2.5 obtained by adding HCl. This medium was chosen to have a better stability of the films. Finally, the electrochemical studies were carried out in the same medium.

The film behaviour was investigated first by cyclic electrogravimetry and then by *ac*-electrogravimetry. *Ac*-electrogravimetric measurements were carried out by using a 4 channels

frequency response analyser (Solartron 1254 TFA) and home-made potentiostat and quartz crystal microbalance. Details of the experimental equipment are given elsewhere [17, 41, 42] Films are considered as acoustically thin enough and this hypothesis is fully justified with PB film thickness in the sub-micrometric range [43]

The PB films were tested in various conditions in aqueous media, 0.5 M KCl at pH 2.5, 0.05M KCl at pH 5.4, and then, the influence of KCl concentration at pH 5.4 was investigated.

4 - RESULTS

4.1- Investigation of PB films in 0.5 M KCl at pH 2.5

4.1.1. - *Cyclic electrogravimetry*

The PB film behaviour was studied in the potential domain where the PB↔ES conversion occurs (Equation 1). Figure 2 presents the changes of mass and current in a -0.2V à 0.6V vs SCE (Saturated Calomel Electrode) potential range obtained at the 15th cycle for a PB film immersed in 0.5M KCl at pH 2.5. So, the electronic charge transfer at the film/electrode interface (change of the current) can be correlated to the ionic transfer at the film/electrolyte interface (change of the mass). The mass increased during the reduction and decreased during the oxidation. This confirms that the film electroneutrality was maintained by cation participation as it has been already shown that K^+ ions mainly participate to the charge compensation in the negative potentials range whereas protons, H_3O^+ and H^+, are mainly involved towards the positive potentials [44].

4.1.2– *Study of the PB film at 0.175 V vs SCE*

Ac-electrogravimetric measurements on a PB film were carried out in 0.5M KCl - pH 2.5 at various potentials. At each imposed potential, the mass, $\Delta m(\omega)$, and the current, $\Delta I(\omega)$, responses of the film to a potential sinusoidal perturbation of low amplitude $\Delta E(\omega)$ (50mV) were measured at various modulation frequencies between 63kHz and 10mHz by using a four channels frequency response analyser. This value of amplitude was selected as it is a good trade-off between linearity and accuracy.

As an example, the full data processing of the experimental data obtained on the PB film polarized at 0.175 V vs SCE is first given. Figure 3 shows the three principal transfer functions, two experimental $\frac{\Delta E}{\Delta I}(\omega)$ and $\frac{\Delta m}{\Delta E}(\omega)$ and another one calculated $\frac{\Delta q}{\Delta E}(\omega)$, of a PB film at 0.175V vs. SCE. Based on the model described above, the three transfer functions

were separately fitted under WINCLNSF and the estimated parameters are given in Figure 2d. The electrochemical impedance $\frac{\Delta E}{\Delta I}(\omega)$ (Figure 3a) had the classical shape of the behaviour of a blocked electrode with a quasi-vertical capacitive part in the low frequency range. By considering a global ionic transfer, the electronic transfer resistance, R_e = 0.89 Ω was shown to be lower than the global ionic transfer resistance, R_t = 22 Ω. This demonstrates that ionic transfer at the film/electrolyte interface limits the kinetics of the film reduction or oxidation. At last, a value of 1.5 Ω cm was obtained for the pore resistivity of the electrolyte in the film. In addition, this result shows that electronic transfer is fast as it responds in the high frequency range, between 63 kHz and 1 kHz. Ionic transfer is slower as it responds in the low frequency range and it occurs at the pore surface with a potential distribution along the pore.

The second transfer function, $\frac{\Delta q}{\Delta E}(\omega)$**,** which is calculated by using the experimental data of the electrochemical impedance (eq. 42), is shown in Figure 3b. The two, not well separated, loops displayed at this potential pointed out that there are two charged species involved in the film redox process. This can be either two cations or two anions or one cation and one anion. A fitting procedure based on Equation (43) allowed the ionic transfer resistance and the insertion capacity of each ion to be estimated and then the kinetic parameters K_i and G_i (Figure 3d).

The electrogravimetric transfer function, $\frac{\Delta m}{\Delta E}(\omega)$, also displays two loops (Figure 3c). They are located in the third quadrant which corresponds to the expulsion of two cations during the film oxidation. After the fitting procedure based on Equation (47) the atomic masses of the involved cations are determined, their values show that the two detected cations are the potassium (m_{c1} = 39 g.mole^{-1}) related to the slowest process (K_{c_1}) and the hydronium (m_{c2} = 19 g mole^{-1}) related to the fastest process (K_{c_2}). This means that the H_3O^+ transfer kinetics is faster than the K^+ transfer. The two cations participate in the same direction to the charge compensation. They are expulsed towards the electrolyte during the film oxidation and are inserted in the film from the electrolyte during the film reduction with well-defined kinetics for each ion. It is the first time that the separate contribution of the two involved species is demonstrated and that their kinetics are clearly determined.

4.1.3 – *Study of the PB film behaviour with respect to the potential*

In a similar way, fittings were carried out for all the analysed potentials between 0 and 0.325V vs. SCE. Figure 4a shows the variation of the electronic transfer resistance, R_e, and of the ionic transfer resistance, R_t, obtained from the electrochemical impedance at each potential. They show a minimum at the potentials where the PB↔ES conversion occurs. In addition, the ionic transfer resistance is always higher than the electronic transfer resistance whatever the imposed potential to the PB film. This means that the kinetics of the global charge transfer of the PB film is controlled by ionic transfer during a redox process whatever the potential. However, the ionic transfer resistance, R_t, obtained from the impedance is a global resistance for all the charged species involved in the electrochemical process. Moreover, the pore resistivity, ρ_2, changes with respect to the potential (Figure 4b) with a minimum, in the vicinity of the PB↔ES conversion potential, which could have two origins. On the one hand, the impoverishment of cations in the pore when going towards negative potentials, where cations enter the film, leads to an increase of the resistivity. On the other hand, the change of the zeolitic structure related to the lattice contraction when the film is oxidized induce an increase of the pore resistivity due to the decrease of the pore diameter.[45, 46]

The K_c and G_c kinetic constants, are plotted on Figure 4 with respect to the potential. G_c is greater for K^+ than H_3O^+ for whatever the imposed potential. In addition, the quantity dC_c / dE, which is the derivative of the concentration with respect to the imposed potential, for each species, can be calculated by considering the low frequency limit of $\frac{\Delta C_i}{\Delta E}(\omega)$, then:

$$\frac{\Delta C_i}{\Delta E}(\omega) = \frac{-G_i}{j\omega d_f + K_i} \rightarrow \frac{\Delta C_i}{\Delta E}(0) = -\frac{G_i}{K_i} \qquad (48)$$

The variation of this quantity for the two cations K^+ and H_3O^+, is shown on Figure 4e with respect to the potential. dC_c / dE reaches a maximum at the potential of the PB↔ES conversion. This corresponds to the maximum of the current of the cyclic voltammogram (Figure 2).

The change of the relative concentration in the film of each cation can be calculated with respect to the potential by integrating the quantity dC_c / dE. Figure 4f shows that the relative concentration of the species in the film decreases when the potential becomes more anodic. The negative sign means that the cation is expulsed from the film during its oxidation. The K^+ concentration change between the two states, reduced and oxidized, (ΔC_{c1} = 3.3 mmole.cm^{-3}) is greater than the concentration change of H_3O^+ (ΔC_{c2} = 1.4 mmole.cm^{-3}). So,

H_3O^+ contributes by 33.6 % to the total flux of the species exchanged between 0 and 0.35V vs. SCE. This demonstrates that K^+ plays a greater role than H_3O^+ in the charge compensation process.

4.2 - Investigation of PB films in 0.05 M KCl 0.05M at pH 5.4

4.2.1 - *Cyclic electrogravimetry*

When the film was converted under the soluble form by applying 15 consecutive cycles in 0.5M KCl -pH 2.5, the investigation of the redox properties of the PB film was carried out in a 0.05M KCl - pH 5.4 aqueous medium.

Figure 5 shows the shapes of the current-potential and mass-potential curves. They are similar as those plotted in the 0.5M KCl – pH 2.5 aqueous medium (Figure 2). However, the redox peak occurs at a more cathodic potential, around 0.1V vs. SCE. The charges estimated between the two pH values are in the same order of magnitude as mainly related to the electronic transfer and indirectly connected to the ionic transfers in term of kinetics. In addition, the mass change between the reduced and oxidized states is smaller (1.5 µg cm^{-2}) than at pH 2.5 and the sense of variation shows that, like at pH 2.5, the reversible PB↔ES conversion is mainly due to cations transfer.

4.2.2 - *Ac-Electrogravimetry*

As previously, the three transfer functions were obtained for the PB film in 0.05M KCl at pH 5.4 between -0.1 V and 0.35 V vs SCE. Then, the fitting procedure was used.

The shapes of the three transfer functions were very close to those obtained at pH 2.5. By using the model of the porous electroactive film given previously, the fitting procedure was applied separately on each transfer function for all potentials. With this model, it is noticeable that a good agreement can be found between the experimental and the calculated diagrams. The electrochemical impedance has still a shape similar to the one of a blocking electrode. The charge/potential transfer function presents two loops corresponding to the relaxations of the two cations K^+ and H_3O^+. The electrogravimetric transfer function shows the presence of a third species.

The analysis of the electrochemical impedance gives information on the charge transfer of the PB film during the electrochemical process. Like at pH 2.5, the rate limiting step of the global charge transfer is the ionic transfer at the film/electrolyte interface as the value of the ionic transfer resistance, R_t, is always larger than the resistance corresponding to

the electronic transfer, R_e, whatever the potential applied to the PB film (Figure 6a). However, at pH 5.4, the process is slower as the resistances R_t and R_e determined for 0.05M KCl at pH 5.4 are much larger than those determined for 0.5M KCl at pH 2.5 (Figure 4a). This can be explained by the decrease of both the KCl and protons concentration for 0.05M KCl at pH 5.4. The resistivity of the pore (Figure 6b) also changes with both concentrations and potential and it is higher for 0.05M KCl at pH 5.4. This is mainly due to a higher resistivity of the solution at pH 5.4 (R_s = 32 Ω) than at pH 2.5 (R_s = 3.8 Ω).

The fitting of the experimental electrogravimetric transfer function $\frac{\Delta m}{\Delta E}(\omega)$ allows the values of the kinetic constants K_c and G_c to be determined. The estimated atomic masses $m_{c_1} = 39$ g mole^{-1}, $m_{c_2} = 19$ g mole^{-1} and $m_s = 18$ g mole^{-1} show that the third involved species is the solvent. These quantities are plotted with respect to the potential in Figure 6c and d. Like at pH 2.5, H_3O^+ insertion is the fastest process as the quantities K_c, which is the time constant of the cation movement is larger for H_3O^+ than for K^+ and the solvent.. Nevertheless, the constants G_c for K^+ and H_3O^+ are smaller for 0.05M KCl at pH 5.4. Moreover, the fitting for the electrochemical impedance points out that the global ionic transfer resistance, R_t, of the two cations K^+ and H^+ is larger at pH 5.4, which leads to an average constant G_t smaller than at pH 2.5 from the relationship $G_t = 1/96500R_t$. Consequently, the constants K_c and G_c associated to the K^+ and H_3O^+ ions are smaller and are correlated to the K^+ and H^+concentrations.

The change of the derivatives of the insertion law for the K^+ and H_3O^+ ions are given in Figure 6e with respect to the potential. The value of dC_c / dE reaches a maximum at the potential where the PB↔ES conversion occurs. This is in good agreement with the cyclic electrogravimetric curve (Figure 5). The ratio between the two values of dC_c / dE for K^+ and H_3O^+ is larger at the negative potentials between 0.0V and 0.2V (Figure 6e). This means that the role of the K^+ ion is predominant at negative potentials whereas the role of H_3O^+ is predominant at positive potentials. Nevertheless, the same conclusion was reached when only one global insertion rate, $K_{c,}$, was considered for an apparent average mass of K^+ and H_3O^+ [17] as the apparent mass of the positive species is larger at negative potentials than at positive potentials.

The change of the concentration, in the PB film between the reduced and oxidized states, of K^+ (ΔC_{c1} = 3.4 mmole cm^{-3}) is larger than the one for H_3O^+ (ΔC_{c2} = 0.7 mmole cm^{-3}). So, 17.0 % of H_3O^+ contributes to the total flux of the exchanged species between -0.05

and 0.35V vs. SCE. This means that the K^+ ion plays a more important role than the H_3O^+ ion in the charge compensation during the redox switching of the PB film. As there is less protons at pH 5.4 than at pH 2.5, it is normal that the quantity of implied H_3O^+ ions is lower at pH 5.4.

4.3 - Influence of the KCl concentration at pH 5.4

The influence of the KCl concentration in aqueous solutions at pH 5.4 on the electrogravimetric response of a PB film was studied. The soluble PB film was preconditioned in 0.1M KCl during one hour. The electrochemical measurements were carried out on the same film by increasing the KCl concentration from 0.01M to 0.5M. At each concentration, the cyclic electrogravimetric measurement was carried out during three cycles in order to obtain a well equilibrated film before the ac-electrogravimetric measurements carried out at a potential 0.25V vs. SCE.

4.3.1 - *Cyclic electrogravimetry*

The current-voltage curves are given in Figure 7a for various KCl concentrations. The anodic redox peak related to the PB↔ES conversion shifts towards more positive potentials when the KCl concentration increases. The change of the potential of the cathodic peak is more important than the change of the anodic peak when the KCl concentration varies from 0.01M to 0.5M. This dissymmetry of the current responses to the cathodic and anodic potential sweeps can be explained by considering that cationic transfer occurs on the one hand from the film, where the cations concentration is independent of the solution, for the anodic sweep and on the other hand from the solution, where cation concentration changes, towards the film, for the cathodic sweep. For this reason, the current response is more influenced by the cation concentration in the solution when the potential decreases.

In addition, the electrochemical processes are more reversible at high concentration because the two potentials of the anodic (E_a) and cathodic (E_c) peaks are closer (Table 1). This indicates also that ionic transfer at the film/solution interface is probably the major limiting process for the redox switching of the PB film in KCl aqueous media compared to electronic transfer at the electrode/film interface.

The two potentials of the anodic and cathodic peaks allow the formal potential ($E_{p\text{-}p}$) to be calculated at each concentration (Table 1) following the equation:

$$E_{p-p} = \frac{E_a + E_c}{2} \tag{49}$$

The linear fitting of the formal potential, $E_{p\text{-}p}$, with respect to the logarithm of the KCl concentration gives a value of 43 mV/decade of KCl concentration. This value is rather far from the theoretical value (59 mV/decade) given by the Nernst equation. If the redox process is supposed to be due to the potassium participation, the value 43 mV/decade corresponds to the PB↔ES reaction with a K^+ cation for a reduced Fe^{3+} ion.

From the *i-E*, curve, the anodic (Q_a) and cathodic (Q_c) charges were determined as well (Table 1). In spite of the fact that the anodic and cathodic peaks are not at the same potential, the anodic and cathodic charges are almost equal at each concentration. This means that the redox process related to the PB↔ES reaction is reversible whatever the studied concentration.

The mass differences between the two potentials -0.2V and 0.6V vs. SCE (Figure 7b) are practically equal (1.3 $\mu g.cm^{-2}$) whatever the KCl concentration and the direction of the potential sweeping. This mass difference is proportional to the charge by assuming that the reaction process is only due to the cations participation (K^+ and H_3O^+). This confirms the hypothesis of a reversible reaction process in the -0.2V and 0.6V potential range.

However, the slope of the *Δm-E* curves changes with the concentration. From the *Δm-E* curve plotted at each concentration, the slope of the cyclic *Δm/ΔE* can be estimated and will be compared below with the low frequency value of $\Delta m / \Delta E(\omega)$ obtained from the *ac*-electrogravimetric experiments. In fact, in the zone between 0.2 and 0.3V vs. SCE, the change of mass is practically linear, in the two directions, anodic, $\Delta m/\Delta E_a$, and cathodic, $\Delta m/\Delta E_c$ (Table 1). However, a discrepancy can be observed between the cathodic and anodic values at each concentration. This dissymmetry is due to the fact that the PB film response is more influenced by the KCl concentration in the reduction direction than in the oxidation direction. However, these values increase with the KCl concentration whatever the direction of the sweeping potential.

4.3.2 - *Ac-electrogravimetry*

4.3.2.1 - Electrochemical impedance

The response of the electrochemical impedance of the PB film at 0.25V vs. SCE at various KCl concentrations is shown in Figure 8a. First, the size of the high frequency capacitive loop decreases when the KCl concentration increases. This implies that ionic

transfer is facilitated. The fitting procedure allows the various parameters which characterize the global charge transfer of the film to be calculated. The two transfer resistances R_e and R_t decrease when the KCl concentration increases (Figure 8b). This demonstrates an acceleration of the processes when the KCl concentration increases. In addition, the global charge transfer process is always controlled by ionic transfer as the ionic resistance is always larger than the electronic resistance whatever the studied KCl concentration (Figure 8c). However, the ratio between R_t and R_e decreases when the KCl concentration increases. This means that, when KCl concentration increases, as ionic transfer is accelerated the global charge transfer is more and more controlled by electronic transfer.

The fitting of the electrochemical impedance diagram also allows the pore resistivity, ρ_2, to be calculated (Figure 8d). This quantity decreases when the KCl concentration increases, due to the increase of the conductivity. Hence, it is correlated with the electrolyte conductivity characterized by R_s.

4.3.2.2 - Mass-potential transfer function

Figure 9a compares the electrogravimetric transfer functions, $\Delta m / \Delta E(\omega)$, for a PB film polarized at 0.25V vs. SCE at various KCl concentrations. The loops, which are located in the third quadrant, correspond predominantly to cation insertion. In fact, the increase of the KCl concentration favours the species insertion at the film/solution interface and consequently, the size of the $\Delta m / \Delta E(\omega)$ loop increases with the KCl concentration. The fittings were carried out as previously by considering the two cations K^+ and H_3O^+ and the solvent.

It is noticeable that the point measured at 0.025 Hz of the electrogravimetric curves in the aqueous solution at pH = 5.4 corresponds roughly to a 20 $mV.s^{-1}$ scan rate on a 0.8 V sweeping range in cyclic electrogravimetry. It should be point out that the role of H_3O^+ is preponderant at this frequency.

The $\left|\frac{\Delta m}{\Delta E}\right|$ values extracted from the ac-electrogravimetric curves increase with the KCl concentration (Table 2). Additionally, by comparing with the calculated values obtained from the cyclic electrogravimetry they are close to the anodic values for concentrations between 0.15M and 0.5M whereas for more diluted concentrations, between 0.01M and 0.1M, they are close to the cathodic values.

Figure 9b and c show the variations of K_c and G_c for K^+, H_3O^+, and the solvent with respect to the KCl concentration. As the studied media have a pH equal to 5.4, the proton concentration does not change with the increase of the KCl concentration. The kinetic constant K_c of the inserted species do not change very much with the KCl concentration. These results were obtained at 0.25V vs. SCE where the PB film rather favours H_3O^+ insertion compared with the negative potentials (0-0.2V vs. SCE) [17, 44].

The kinetic constant G_i for H_3O^+ and the solvent increase and then become constant with respect to the potential contrarily to the one of K^+ which increases continuously with KCl concentration.

The values of dC_c / dE were also calculated for the three species K^+, H_3O^+ and the solvent. The same evolution of this quantity can be observed for the two cations. The potassium plays a more important role than the hydronium in the charge compensation process because the value of dC_i / dE is larger for K^+ than for H_3O^+. In addition, the ratio $(dC_{H_3O^+} / dE)/(dC_{K^+} / dE)$ decreases with the KCl concentrations (Figure 9d). This means that the role of H_3O^+ is less and less important for the large KCl concentrations as dC_c / dE is related to the facilities of the ion insertions. At this potential, the process is more and more limited by the kinetics of the potassium ions.

5 - DISCUSSION

The kinetics of the electrochemical process of the PB film in KCl media is mainly controlled by ionic transfer at the film/solution interface. It is mainly related to the participation of two cations, K^+ and H_3O^+, which was already suggested, especially at low pH, for the reaction mechanisms in the literature [12, 16, 47] The soluble and hydrated PB films contain about 14 to 16 water molecules for a mesh unit. Although water movement is clearly detected only for pH 5.4, the water located in the interstitial sites of the hydrated structure of PB can play a very important role for the cations K^+ and H_3O^+ movement whatever the pH value. Gimenez-Romero et al. [48] have proposed the following mechanism for the insertion reaction of the cations K^+ and H_3O^+ in a PB film, $K_h Fe_k^{3+}\left[Fe^{2+}(CN)_6\right]_l .mH_2O$ by considering the dual insertion mechanism:

$$K_h Fe_k^{3+}\left[Fe^{2+}(CN)_6\right]_l .mH_2O + nK^+_{solution} + ne^- \underset{\leftarrow}{\overset{\rightarrow}{}} K_{h+n} Fe_{k-n}^{3+} Fe_n^{2+}\left[Fe^{2+}(CN)_6\right]_l .mH_2O \quad (50)$$

$$K_h Fe_k^{3+}\left[Fe^{2+}(CN)_6\right]_l .mH_2O + nH_3O^+_{solution} + ne^- \overrightarrow{\leftarrow}$$
$$K_h Fe_{k-n}^{3+} Fe_n^{2+}\left[Fe^{2+}(CN)_6\right]_l .mH_2O\left(nH_3O^+\right) \quad (51)$$

The authors have suggested that the hydrated PB film contains a hydrated part, mH_2O and another part with crystalline structure, $K_h Fe_k^{3+}\left[Fe^{2+}(CN)_6\right]_l$. The mH_2O part occupies interstitial sites which are located in channels of the hydrated structure $K_h Fe_k^{3+}\left[Fe^{2+}(CN)_6\right]_l .mH_2O$. During the PB↔ES transition, The K^+ movement is accompanied by the existing water molecules in the structure $K_h Fe_k^{3+}\left[Fe^{2+}(CN)_6\right]_l .mH_2O$ although the H_3O^+ movement occurs in the channels of this structure in order to maintain the film electroneutrality. This insertion mechanism of the cations K^+ and H_3O^+ in independent sites is in agreement with the results obtained by *ac*-electrogravimetry and it is noticeable that no movement of free water through the film/solution interface was detected at low pH showing that water molecules stay in the film during the redox process. For higher pH water movement was demonstrated in agreement with results published in the literature [49,50] In these conditions both water bounded to the protons and free water cross this interface. This difficulty of water transport at low pH is probably due to the fact that PB is an ionic crystalline solid, that is, a rigid structure [51] Obviously, this differs greatly from polymer electroactive film where the solvent molecules may contribute to the mass change during redox switching [52], particularly for polypyrrole [53] and polyaniline [38].

6 - CONCLUSIONS

The study of the PB film in a KCl medium at pH 2.5 and 5.4 was carried out in this work. A theoretical model based on a porous film and which distinguishes electronic and ionic charge transfer was applied for the first time to interpret the experimental results obtained through *ac*-electrogravimetry.

The electrochemical impedance gave information on the global charge transfer kinetics which is controlled by ionic transfer for the whole potential range imposed to the PB film and whatever the KCl concentration as the resistance associated to the electronic transfer is lower than the resistance associated to the ionic transfer. However, electronic transfer becomes more and more limiting when the KCl concentration increases when the film behaviour is studied at 0.25 V vs. SCE. Moreover, the rates of the electronic and ionic transfer

kinetics vary with the potential. They are faster around the potential where the PB↔ES conversion occurs. The resistances associated to the electronic and ionic transfers present a minimum in this zone compared to the more anodic or negative potentials. The second information extracted from the impedance concerns the porosity of the PB film which is related to the zeolitic nature of the film. The resistivity of the pore depends on the potential and obviously on the electrolyte conductance.

Ac-electrogravimetry gave essentially information on the kinetics of the ionic transfer. Thanks to the model of electroactive porous films and the digital fitting procedure, for the first time, the two cations K^+ and H_3O^+ are identified with well separated kinetics for each cation. When a potential is applied to the PB film, the H_3O^+ ion transfer is faster than the K^+ ion transfer. Nevertheless, K^+ ions play a more important role than H_3O^+ in the charge compensation process whatever the pH and the KCl concentration or the applied potential. However, the role of H_3O^+ decreases for the higher KCl concentrations (between 0.1 M and 0.5 M) when the film is studied at pH = 5.4 and for an imposed potential equal to 0.25 V. Water movement was only detected for the highest pH. For low pH, water was blocked in the PB structure. Now, perspectives can be considered in term of structural changes which can accompanied the ion/solvent transfer. For that, a coupling between *ac*-electrogravimetry and XRD analysis seems an attractive direction to examine this idea.

C_M (mole l^{-1})	log(c_M)	E_a (V)	E_c (V)	E_{p-p} (V)	Q_c (mC cm^{-2})	Q_a (mC cm^{-2})	$\Delta m/\Delta E_c$ (µg cm^{-2} V^{-1})	$\Delta m/\Delta E_a$ (µg cm^{-2} V^{-1})
0.01	-2	0.177	0.011	0.094	4.177	4.092	-0.584	-3.061
0.05	-1.3	0.154	0.090	0.122	4.060	3.950	-0.98	-2.566
0.1	-1	0.16	0.116	0.138	3.963	3.861	-1.266	-2.804
0.15	-0.83	0.166	0.128	0.147	3.909	3.782	-1.39	-2.985
0.25	-0.6	0.168	0.134	0.151	3.856	3.690	-1.535	-3.099
0.5	-0.3	0.182	0.154	0.168	3.797	3.641	-1.877	-3.604

Table 1: Parameters estimated from cyclic electrogravimetric curves with respect to the KCl concentration.

C_M (mole.l^{-1}) / µg cm^{-2} V^{-1}	**0.01**	**0.05**	**0.1**	**0.15**	**0.25**	**0.5**
$\Delta m/\Delta E_c$	-0.584	-0.98	-1.266	-1.39	-1.535	-1.877
$\left(\frac{\Delta m}{\Delta E}\right)_{0,025Hz}$	-1.087	-1.837	-2.278	-2.567	-3.020	-3.805
$\Delta m/\Delta E_a$	-3.061	-2.566	-2.804	-2.985	-3.099	-3.604

Table 2 : $\left|\frac{\Delta m}{\Delta E}\right|$ values at 0.025 Hz of the PB film at 0.25 V vs. SCE. and comparison with $\Delta m/\Delta E$ obtained in cyclic electrogravimetry.

FIGURE CAPTIONS

Figure 1: Diagram of the proposed porous model.

Figure 2: Cyclic voltammogram and electromassogram for a PB film in 0.5M KCl at pH 2.5 plotted for the 15th cycle. Potential sweep between -0.2V and 0.6V vs. SCE with a 20 mV.s^{-1} sweeping rate.

Figure 3: Experimental and theoretical transfer functions (a, b, c) with the following estimated parameters at 0.175V vs. SCE for a PB film in 0.5M KCl at pH 2.5.

Figure 4: Variations of R_e, R_t (a), ρ_2 (b), K_c (c), G_c (d), $dC_c(E)/dE$ (e) and of the relative concentration of the species ΔC_c (f) with respect to the potential. Calculations were carried out from $\Delta E / \Delta I(\omega)$ and $\Delta m / \Delta E(\omega)$ functions for a PB film in 0.5M KCl at pH 2.5.

Figure 5: Cyclic electrogravimetry of the redox behaviour of a PB film (a) in 0.05M KCl at pH 5.4 obtained at the 10th cycle with a potential scan between -0.2V and 0.6V vs. SCE and a 20 mV.s^{-1} sweep rate.

Figure 6: Variation with respect to the potential of K_c (a) G_c (b), dC(E)/dE (c) and of the change of the concentrations of species ΔC_c in the PB film (d) calculated from the transfer functions $\Delta E / \Delta I(\omega)$ and $\Delta m / \Delta E(\omega)$ for a PB film in 0.05M KCl at pH 5.4.

Figure 7: Cyclic electrogravimetric curves: *i-E* (a) and *Δm-E* (b), for a PB film cycled between -0.2 and 0.6V vs. SCE with a 20 mV s^{-1} sweeping rate, for various KCl concentrations.

Figure 8: Diagrams of the electrochemical impedance (a) and variations of R_e and R_t (b), R_t/R_e (c), ρ_2 and R_s (d) with respect to the KCl concentration for a PB film immersed in an pH 5.4 aqueous medium at 0.25V vs SCE.

Figure 9: Electrogravimetric transfer function (a) and variation of Kc (b), Gc (c) and dC_c / dE at 0.25V vs. SCE, with respect to the KCl concentration at pH 5.4.

REFERENCES

[1] D. Ellis, M. Eckhoff; V. D. Neff, J. Phys. Chem. 85 (1981) 1225.
[2] K. Itaya, H. Akahoshi, S. Toshima, J. Electrochem. Soc., 129 (1982) 762.
[3] K. Itaya, T. Ataka; S. J. Toshima, J. Am.Chem.Soc., 104 (1982) 3751.
[4] H. Kellawi, D. R. Rosseinsky, J. Electroanal. Chem., 131 (1982) 373.
[5] V. D. Neff, 125 (1978) 886.
[6] J. F. Keggin; F. D. Miles, 137 (1936) 577.
[7] H. J. Buser, D. Schwarzenbach, W. Petter, A. Ludi, Inorg. Chem. 16 (1977) 2704.
[8] F. Herren, P. Fischer, A. Ludi, W. Haelg, Inorg.Chem., 19 (1980) 956.
[9] B. Bal; S. Ganguli, M. Bhattacharya, J. Phys.l Chem., 88 (2002) 4575.
[10] K. Itaya, T. Ataka, S. Toshima,. J.Am.Chem.Soc. 104 (1982) 4767.
[11] J. J. Garcia-Jareno, A. Sanmatias, F. Vicente, C. Gabrielli, M. Keddam, H. Perrot, Electrochim.Acta, 45 (2000) 3765.
[12] B. J. Feldman, O. R. Melroy, J. Electroanal. Chem. 234 (1987) 213.
[13] V. Plichon, S. Besbes, J. Electroanal. Chem., 284 (1990) 141.
[14] J. J. Garcia-Jarero, A. Sanmatias, J. Navarro-Laboulais, F. Vicente, Electrochim. Acta, 44 (1998) 395.
[15] J. J. Garcia-Jareno, J. Navarro-Laboulais, F. Vicente, Electrochim. Acta, 41 (1996) 835.
[16] K. Kim, I. Jureviciute, S. Bruckenstein, Electrochim. Acta, 46 (2001) 4133.
[17] C. Gabrielli, J. J. Garcia-Jareno, M. Keddam, H. Perrot, F. Vicente, J. Phys. Chem. B, 106 (2002) 3182.
[18] C. Debiemme-Chouvy, A. Rubin, H. Perrot, C. Deslouis and H. Cachet, Electrochimica Acta., 53, 11 (2008) 3836.
[19] L. To Thi Kim, O. Sel, C. Debiemme-Chouvy, C. Gabrielli, C. Laberty-Robert, H. Perrot and C. Sanchez, Electrochem. Com., 12(2010)1136-1139.
[20] J. Euler, W. Nonnenmacher, Electrochim. Acta, 2 (1960) 268.
[21] R. de Levie, Electrochim. Acta, 8 (1963) 751.
[22] R. de Levie, Electrochim. Acta, 9 (1964) 1231.
[23] R. de Levie, Electrochim. Acta, 10 (1965) 113.
[24] M. Keddam, C. Rakotomavo, H. Takenouti, J. Applied Electrochem., 14 (1984) 437.
[25] J. S. Newman, C. W. Tobias, J. Electrochem. Soc., 109 (1962) 1183.
[26] C. Cachet, R. Wiart, J. Electroanal. Chem., 195 (1985) 21.
[27] O. Bohnke, B. Vuillemin, C. Gabrielli, M. Keddam, H. Perrot, Electrochim.Acta 40 (1995) 2765-2773.
[28] F. La Mantia, J. Vetter, P. Novak, Electrochim. Acta, 53 (2008) 4109.
[29] G. C. Barker, J. Electroanal. Chem. 41 (1973) 201.
[30] W. J. Albery, C. M. Elliott, A. R. Mount, J. Electroanal. Chem., 288 (1990) 15.
[31] R. P. Buck, C. Mundt, J.Chem.Soc., Faraday Trans., 92 (1996) 3947.
[32] T. R. Brumleve, R. P. Buck, J. Electroanal. Chem., 126 (1981) 73.
[33] K. Rosberg, G. Paasch, L. Dunsch; S. Ludwig, J. Electroanal. Chem., 443 (1998) 49.

[34] P. H. Nguyen, G. Paasch, J. Electroanal. Chem., 460 (1999) 63.
[35] G. Paasch, J. Electroanal. Chem., 600 (2007) 131.
[36] C. Ehrenbeck, K. Juttner, S. Ludwig, G. Paasch, Electrochim. Acta, 43 (1998) 2781-2789.
[37] C. Gabrielli, J. J. Garcia-Jareno,H. Perrot, Electrochim. Acta, 16 (2001) 4095.
[38] C. Gabrielli, M. Keddam, N. Nadi, H. Perrot, J. Electroanal. Chem., 485 (2000) 101.
[39] A. Jackson, A. R. Hillman, S. Bruckenstein, I. Jureviciute, J. Electroanal. Chem., 524 (2002) 90.
[40] J. P. Candy, P. Fouilloux, M. Keddam, H. Takenouti, Electrochim. Acta, 27 (1982) 1585.
[41] T. T. L. Kim, PhD thesis, Univ. P. and M. Curie, Paris, France, (2009).
[42] C. Gabrielli, H. Perrot, in Modern aspects of electrochemistry, Vol. 44, p.151-238.
[43] J.J. Garcia-Jareno, C. Gabrielli, and H. Perrot, Electrochem. Com., 2(2000)195-200.
[44] D. Gimenez-Romero, P. R. Bueno, C. Gabrielli, J. J. Garcia-Jareno, H. Perrot, F. Vicente, J. Phys. Chem. B, 110 (2006) 19352.
[45] C. L. Lin, K. C. Ho, J. Electroanal. Chem., 524-525 (2002) 286.
[46] A. Dostal, G. Kauschka, S. J. Reddy, F. Scholz, J. Electroanal. Chem., 406 (1996) 155.
[47] I. Oh, H. Lee, H. Yang, J. Kwak, Electrochem. Comm., 3 (2001) 274.
[48] D. Gimenez-Romero, P. R. Bueno, J. J. Garcia-Jareno, C. Gabrielli, H. Perrot, F. Vicente,.J. Phys. Chem. B, 110 (2006) 2715.
[49] S. J. Lasky, D. A. Buttry, J. Am. Chem. Soc., 110 (1988) 6258.
[50] K. Ogura, M. Nakayama, K. Nakaoka, J. Electroanal. Chem., 474 (1999) 101.
[51] D. Gimenez-Romero, P. R. Bueno, J. J. Garcia-Jareno, C. Gabrielli, H. Perrot, F. Vicente, J. Phys. Chem. B, 110 (2006) 2715.
[52] M. Henderson, A. R. Hillman, E. Vieil, J. Phys.Chem. B, 103 (1999) 8899.
[53] C. Gabrielli, J. J. Garcia-Jareno, M. Keddam, H. Perrot, F. Vicente, J. Phys. Chem. B, 106 (2002) 3192.

- New model of ionic/solvent insertion in electroactive films is developed including porosity.
- Coupling electrochemical impedance and fast quartz crystal microbalance appears as an attractive and powerful technique to investigate electroactive films.
- The separation between potassium and hydronium ions is now possible on PB films.

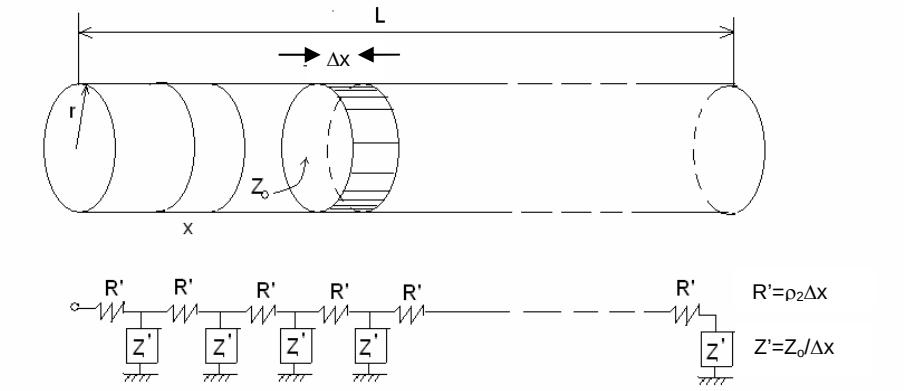
L
Δx
r
Z₀
x
R'
R'
R'
R'
R'
R'
Z'
Z'
Z'
Z'
Z'
R'=ρ₂Δx
Z'=Z₀/Δx

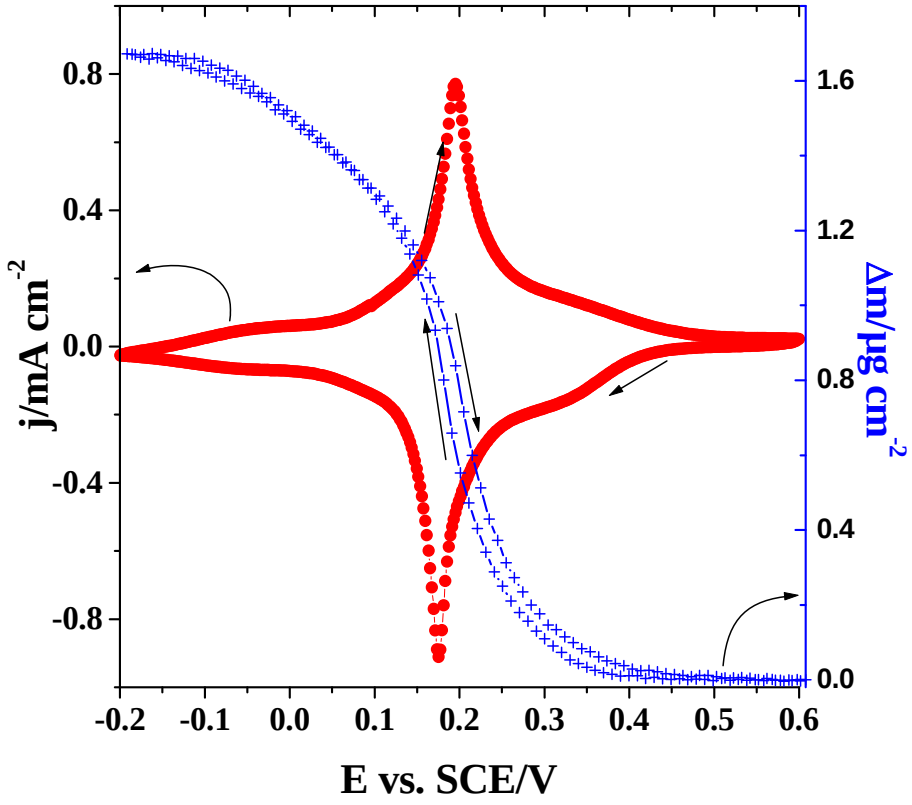
0.8
0.4
0.0
-0.4
-0.8
j/mA cm-2
1.6
1.2
0.8
0.4
0.0
Δm/μg cm-2
-0.2
-0.1
0.0
0.1
0.2
0.3
0.4
0.5
0.6
E vs. SCE/V

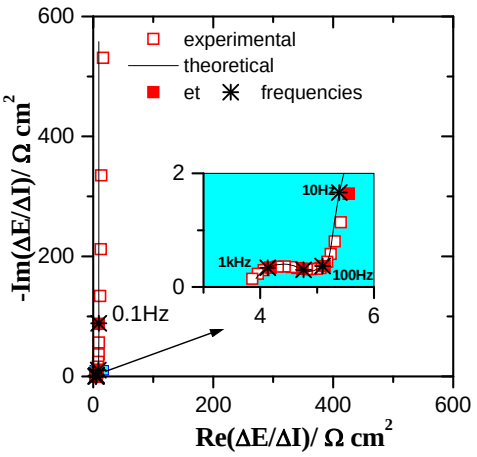

a

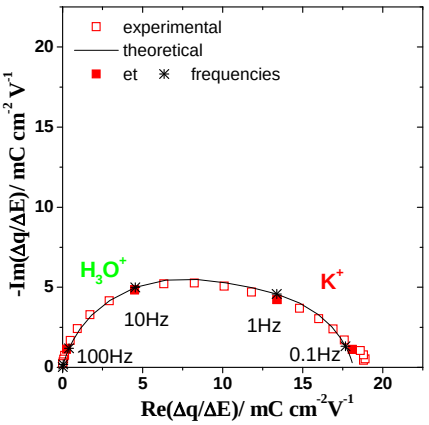

b

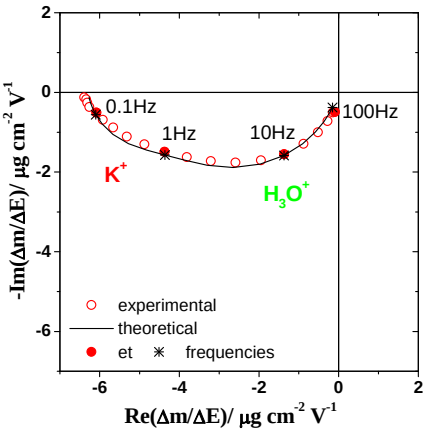

c

Estimated parameter values

Function $\Delta E / \Delta I(\omega)$**:**

C_e = 1.74 10^{-4} F; a_m = 0.95; C_d = 9.6 10^{-3} F;
C_t = 8.4 10^{-3} F; R_e = 0.89 Ω ; R_t = 22 Ω.
ρ_2 = 1.5 Ω cm; R_s = 3.85 Ω.

Function $\Delta q / \Delta E(\omega)$ **:**

K_{c1} = 7.85 10^{-5} cm s^{-1}. G_{c1} = 1.02 10^{-6} mole s^{-1} cm^{-2} V^{-1}. a_{f1} = 0.85
K_{c2} = 1.88 10^{-4} cm s^{-1}. G_{c2} = 1.17 10^{-6} mole s^{-1} cm^{-2} V^{-1}. a_{f2} = 0.85.

Function $\Delta m / \Delta E(\omega)$ **:**

Same values as previously but
m_{c1} = 39 g.$mole^{-1}$. m_{c2} = 19 g $mole^{-1}$.

d

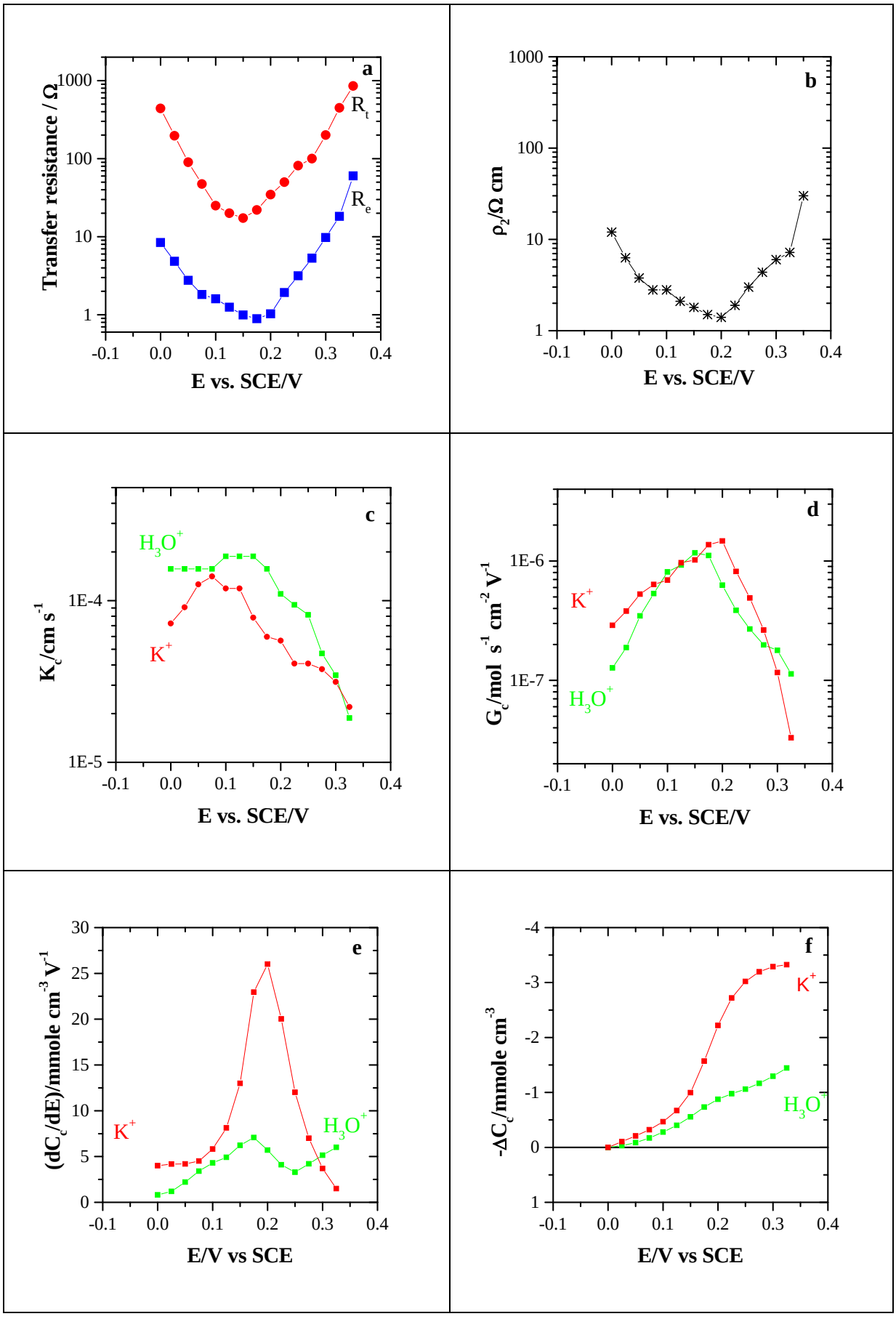
a
Transfer resistance / Ω
1000
100
10
1
R_t
R_e
-0.1
0.0
0.1
0.2
0.3
0.4
E vs. SCE/V
b
ρ_2/Ω cm
1000
100
10
1
E vs. SCE/V
c
K_c/cm s^{-1}
1E-4
1E-5
H_3O^+
K^+
E vs. SCE/V
d
G_c/mol s^{-1} cm^{-2} V^{-1}
1E-6
1E-7
K^+
H_3O^+
E vs. SCE/V
e
(dC_c/dE)/mmole cm^{-3} V^{-1}
30
25
20
15
10
5
0
K^+
H_3O^+
E/V vs SCE
f
$-\Delta C_c$/mmole cm^{-3}
-4
-3
-2
-1
0
1
K^+
H_3O^+
E/V vs SCE

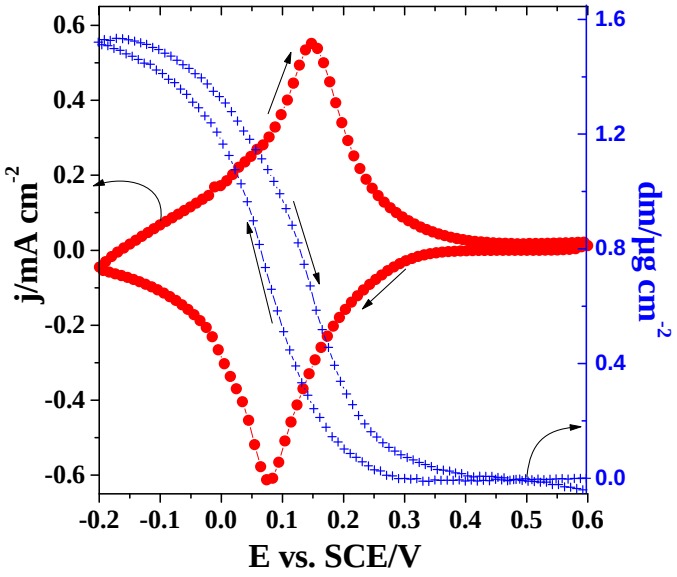
0.6
0.4
0.2
0.0
-0.2
-0.4
-0.6
j/mA cm-2
1.6
1.2
0.8
0.4
0.0
dm/dt gr/ug cm-2
-0.2
-0.1
0.0
0.1
0.2
0.3
0.4
0.5
0.6
E vs. SCE/V

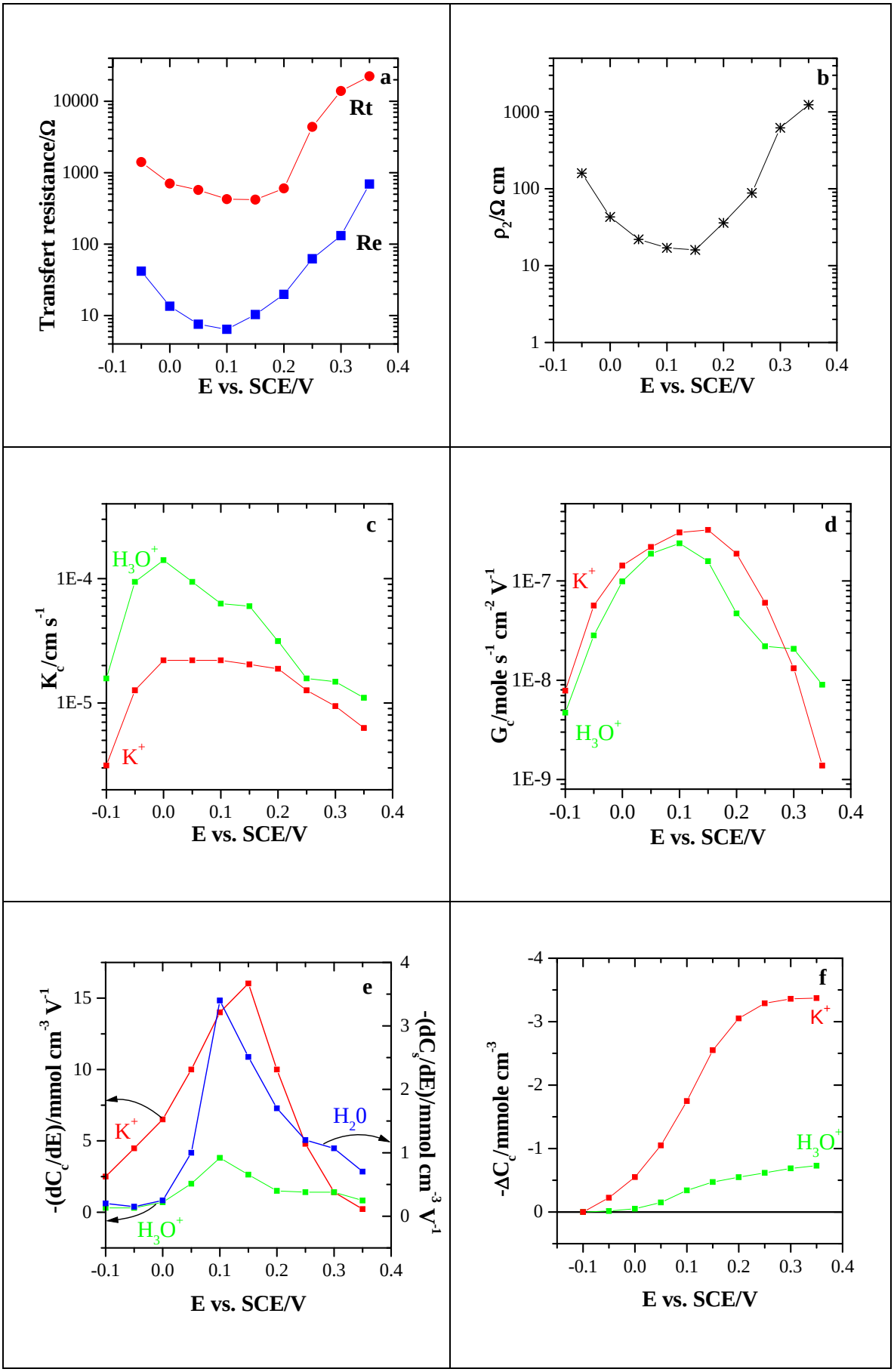
a
Rt
Re
Transfert resistance/Ω
E vs. SCE/V
b
ρ2/Ω cm
E vs. SCE/V
c
H3O+
K+
Kc/cm s-1
E vs. SCE/V
d
K+
H3O+
Gc/mole s-1 cm-2 V-1
E vs. SCE/V
e
K+
H20
H3O+
-(dCc/dE)/mmol cm-3 V-1
-(dCs/dE)/mmol cm-3 V-1
E vs. SCE/V
f
K+
H3O+
-ΔCc/mmole cm-3
E vs. SCE/V

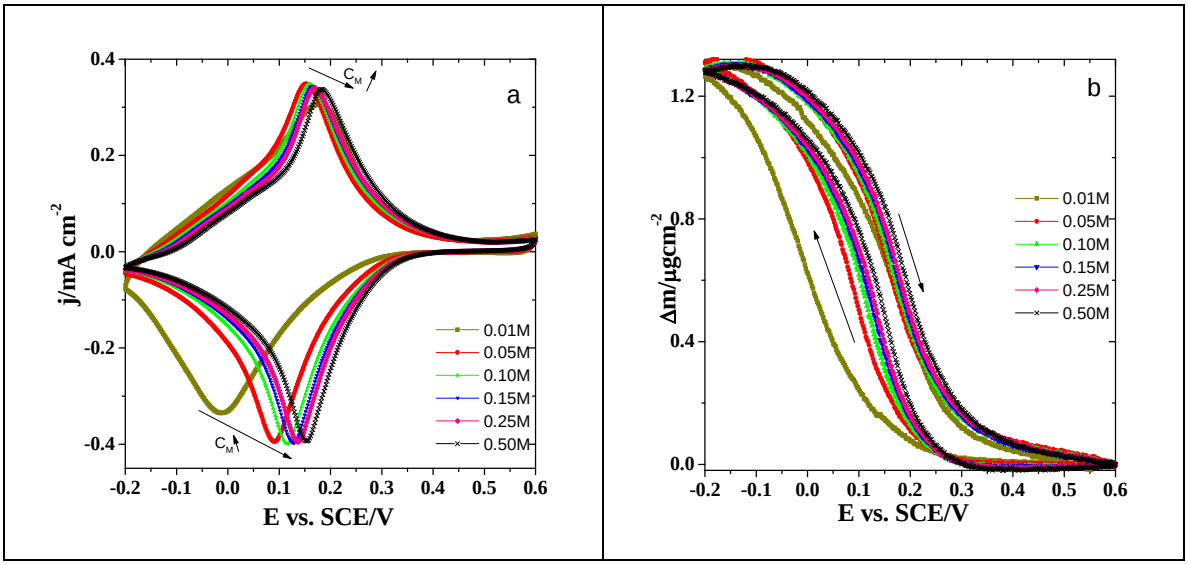
a
b
j/mA cm-2
Δm/μgcm-2
E vs. SCE/V
E vs. SCE/V
CM
CM
0.01M
0.05M
0.10M
0.15M
0.25M
0.50M
0.01M
0.05M
0.10M
0.15M
0.25M
0.50M

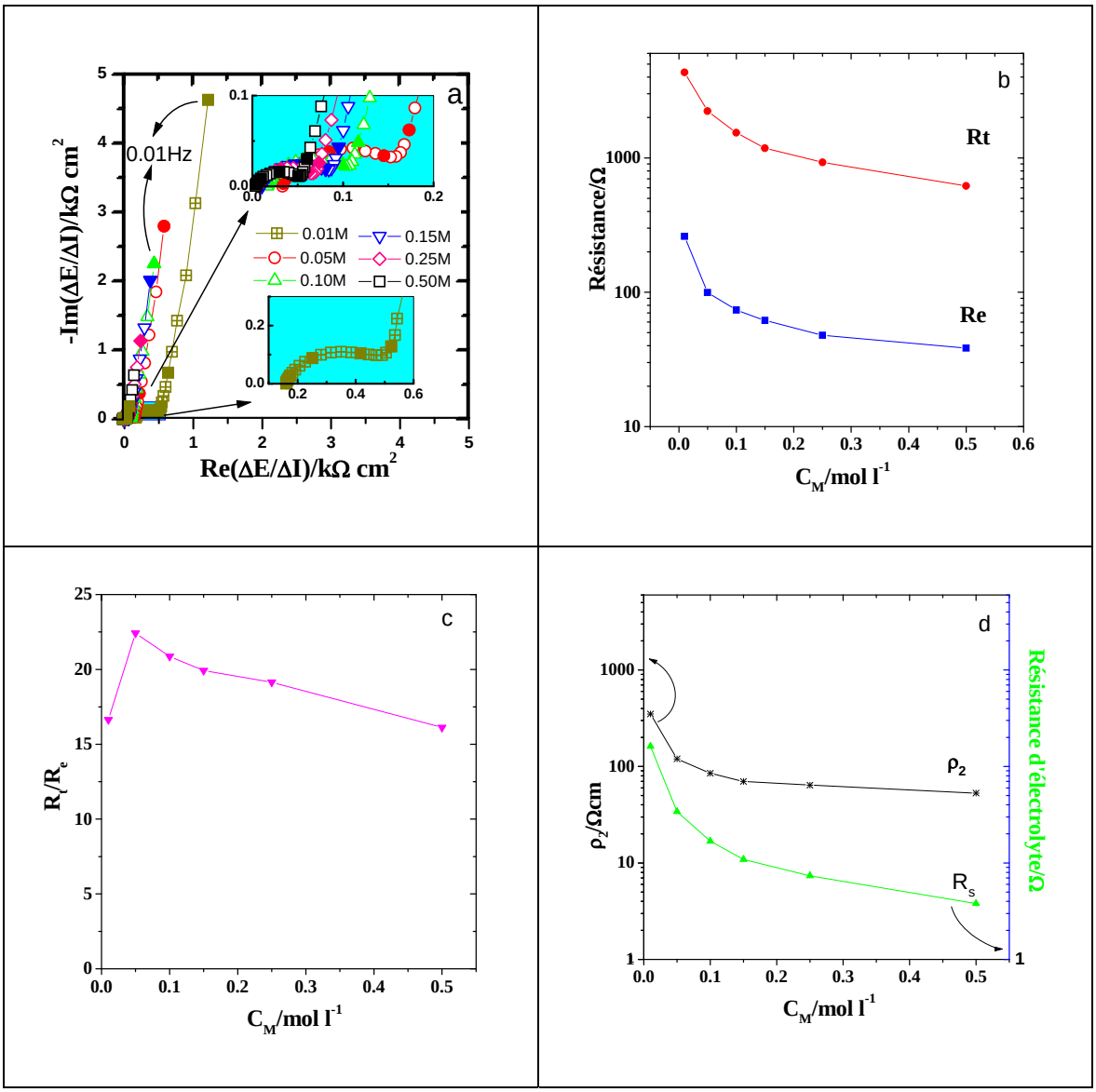
a
0.01Hz
0.01M
0.05M
0.10M
0.15M
0.25M
0.50M
-Im(ΔE/ΔI)/kΩ cm2
Re(ΔE/ΔI)/kΩ cm2
b
Rt
Re
Résistance/Ω
CM/mol l-1
c
Rt/Re
CM/mol l-1
d
ρ2
Rs
ρ2/Ωcm
Résistance d'électrolyte/Ω
CM/mol l-1

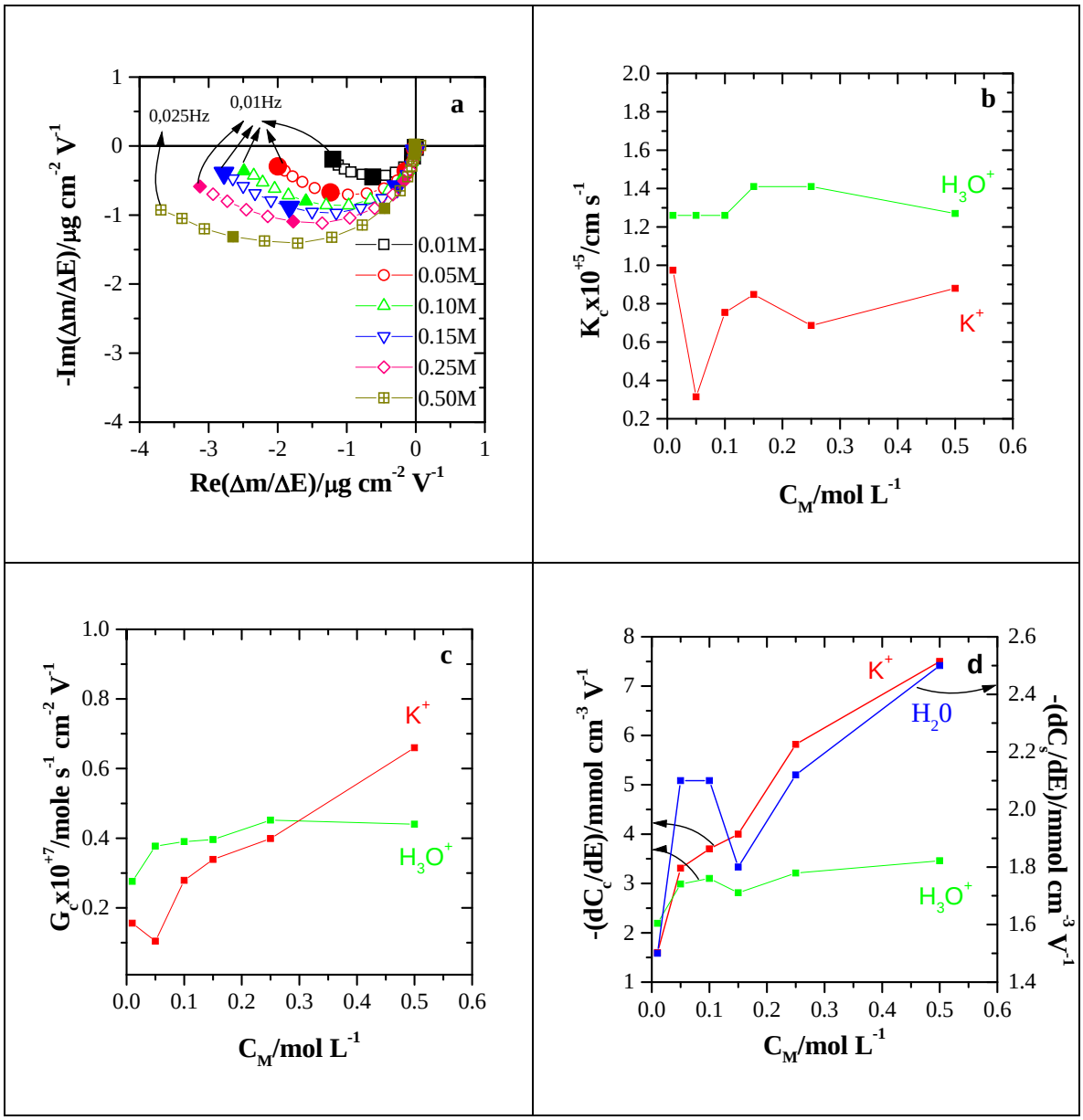
a
0,025Hz
0,01Hz
0.01M
0.05M
0.10M
0.15M
0.25M
0.50M
-Im(Δm/ΔE)/μg cm-2 V-1
Re(Δm/ΔE)/μg cm-2 V-1
b
H3O+
K+
Kc x10+5/cm s-1
CM/mol L-1
c
K+
H3O+
Gc x10+7/mole s-1 cm-2 V-1
CM/mol L-1
d
K+
H20
H3O+
-(dCc/dE)/mmol cm-3 V-1
-(dCs/dE)/mmol cm-3 V-1
CM/mol L-1